第 48 卷 第 7 期/2021 年 4 月/中国激光 研究论文

中国激光

气溶胶微生物粒子计数仪光学系统设计

张志强[1,2]，宋凤民[1]，张秦[3,4]，党磊[3,4]，徐溢[1]，李顺波[1**]，陈李[1,2*]

[1]重庆大学光电工程学院，光电技术与系统教育部重点实验室，新型微纳器件与系统技术重点学科实验室，重庆 400044；

[2]中国科学院传感技术联合国家重点实验室，上海 200050；

[3]航天神舟生物科技集团有限公司，北京 100080；

[4]北京市空间生物工程技术研究中心，北京 100091

摘要 为了实现微生物粒子在线监测，基于荧光探测原理设计了微生物粒子计数仪光学系统。对微生物粒子含有的核黄素、烟酰胺腺嘌呤二核苷酸等物质的荧光特性进行测试和分析，确定了以 405 nm 波长的半导体激光器作为激发光源，提出了荧光检测系统的整体结构。设计了基于组合光阑和透镜组的光源整形光路以及荧光探测光路，以降低光噪声。完成了系统结构的制作和组装。采用荧光微球对检测系统的性能进行了测试，结果表明：系统的输出噪声约为 20 mV，可以实现对粒径为 1，2，5，10 μm 荧光微球的分级检测，具有信噪比高、检测灵敏度高等特点，对进一步开展气溶胶微生物粒子计数仪的研制具有重要意义。

关键词 生物光学；荧光；微生物粒子；光学系统；光噪声

中图分类号 E933.43；Q631 **文献标志码** A **doi**：10.3788/CJL202148.0707002

1 引 言

近年来空气质量愈发受到人们的重视[1-2]，空气中的微生物不仅对人类健康产生了严重危害，也给一些工业生产造成了严重影响[3]。我国最新国家标准《公共场所卫生指标及限值要求》对空气中的细菌总数进行了明确规定。目前，基于荧光技术的微生物检测[4]已被广泛应用于医学、制药、食品[5-6]、环境监测等领域，如实时荧光定量聚合酶链式反应(PCR)[7]、三磷酸腺苷(ATP)荧光检测[8-9]、微生物粒子荧光传感等[10]。荧光微生物粒子计数仪可对微生物粒子进行直接计数，具有实时性好、自动化程度高、操作简便等优点，非常适合空气中微生物浓度水平的实时在线监测。

荧光微生物粒子计数仪采用光散射式检测系统，当微生物粒子经过激发光检测区域时，就会产生荧光脉冲信号，通过探测器检测荧光脉冲就可以实现对微生物粒子的计数。该仪器中最为重要的就是光学检测结构的设计，因为激光光源的输出光斑一般呈高斯分布[11]，光斑中心的能量最强，但周围能量对微弱荧光探测会产生较大影响。此外，光学元件的散射、缺陷等[12-13]会产生一定程度的杂散光[14]，也会对检测结果造成较大影响。

本文对微生物粒子含有的核黄素、烟酰胺腺嘌呤二核苷酸等荧光物质的荧光特性进行了测试和分析。本文以 405 nm 波长的半导体激光器作为激发光源[15-16]，设计了光学检测系统的整体结构。为降低激光器的输出杂散光，本文设计了基于组合光阑和组合透镜的光源整形光路以及荧光探测光路。最后，完成了检测结构的制作和组装，并采用荧光微球对检测系统进行了性能测试。

2 微生物粒子计数仪的工作原理

2.1 微生物粒子的荧光特性

物质发射荧光主要是因为荧光基团吸收光子能量后从最低的电子激发单重态辐射跃迁，从而产生

收稿日期：2020-08-25；**修回日期**：2020-09-29；**录用日期**：2020-10-14

基金项目：国家重点研发计划(2018YFB2002302)、国家自然科学基金(61971074)、民用航天技术预先研究项目(B0107)、中国航天科技集团有限公司自主研发项目(201905)

*E-mail：CL2009@cqu.edu.cn；**E-mail：shunbo.li@cqu.edu.cn

荧光现象[17-18]。微生物体内含有烟酰胺腺嘌呤二核苷酸(NADH)、核黄素[19]等有机分子，这些有机分子在一定波长下被激发时，会发出本征荧光[20]。

本文采用纯度为 98% 的核黄素(分析纯)和 NADH(分析纯)分别进行实验，所使用的仪器均为北京卓立汉光仪器有限公司“影像谱王”系列光栅单色仪/光谱仪以及宁波舜宇仪器有限公司的 CX40 系列正置荧光显微镜。

配制质量浓度为 10.0 μg/mL 的核黄素测试溶液，在蓝光激发下得到核黄素的荧光光谱图，如图 1(a)所示。由图 1(a)可以得知，核黄素在蓝光下激发时，荧光谱的峰值位置为 541 nm。

使用超纯水将 NADH 配制成质量浓度为 600 μg/mL 的 NADH 测试溶液，在蓝光激发下得到其荧光光谱，如图 1(b)所示。由图 1(b)可知，在蓝光激发时，荧光谱的峰值位置为 492 nm。比较图 1(a)、(b)可知，虽然 NADH 的浓度是核黄素的 60 倍，但其荧光强度相对较弱。

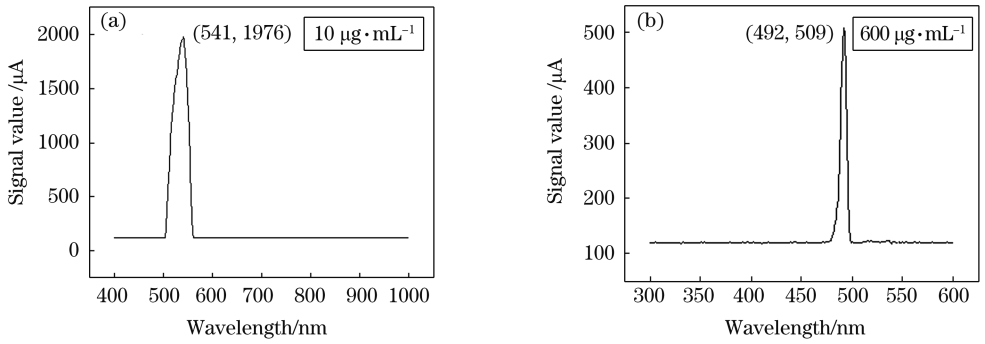

图 1　荧光物质的荧光光谱图。(a) 核黄素溶液的荧光光谱图；(b) NADH 溶液的荧光光谱图

Fig. 1　Fluorescence spectrum of fluorescent substance. (a) Fluorescence spectrum of riboflavin solution; (b) fluorescence spectrum of NADH solution

2.2　微生物粒子光学计数原理

微生物粒子光学计数系统的原理如图 2 所示。采用气泵将待测气溶胶采样到光学检测区，利用一定波长的激发光照射经过光学检测区的气溶胶，微生物粒子中的 NADH、核黄素等发出本征荧光脉冲，通过光电探测器将荧光脉冲转换为电压脉冲信号，且脉冲信号的幅值与粒子的粒径成正相关关系。最后通过信号处理系统对脉冲信号进行统计和分析，即可得到微生物粒子的数量和浓度信息。

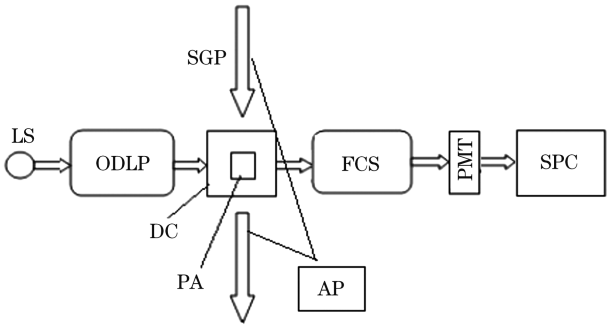

LS: light soutce　PA: photosensitive area
ODLP: optical denoising light path
SGP: sampling gas path　DC: detection cavity
FCS: fluorescence collection system
SPC: signal processing circuit　AP: air pump
PMT:photomultiplier tube

图 2　气溶胶微生物粒子计数仪原理框图

Fig. 2　Principle block diagram of aerosol microbial particle counter

3　光学系统设计

3.1　光路设计

仪器的整体光路结构框图如图 3 所示。检测区 PA 的左侧为激发光源 LS，右侧为光陷阱 LT。在检测区下方设置凹面会聚镜，目的是对微生物产生的荧光信号进行会聚，以提高荧光信号的收集效率。在凹面会聚镜的对面，采用凸透镜组构成的镜头对荧光信号进行采集，经滤光片滤除杂散光后使用凸

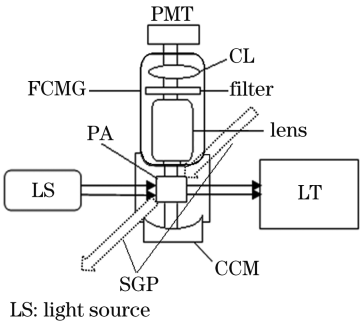

LS: light source
PA: photosensitive area
CCM: concave convergent mirror
LT: light trap
FCMG: fluorescence collection mirror group
CL: convex lens
SGP: sampling gas path

图 3　整体光路结构

Fig. 3　Overall light path structure

透镜进行进一步会聚，照射到光电探测器上的荧光信号被转换为电压脉冲信号。气溶胶采样通路垂直于激发光轴和检测光轴所在的平面。

由于荧光信号非常微弱，为提高系统增益，光电探测器选用光电倍增管（PMT）。为抑制杂散光，PMT 前采用高通滤光片，其下限截止波长是 409 nm，可以很好地滤除 405 nm 的激发杂散光。

3.2　光源整形光路

近年来，405 nm 激光源已商品化，市面上有很多与之相适合的荧光衍生化试剂，而且其波长较短，能够更准确地检测微生物。综合考虑后，本文采用 405 nm 波长的半导体激光器作为激发光源。

首先采用 CCD（电荷耦合器件）对半导体激光器输出光斑进行了测试，测试结果如图 4(a)所示。光斑周围有较强的杂散光，这会极大地降低检测信号的信噪比。为此，本文设计了由光阑和透镜组构成的光源整形光路，如图 5 所示。采用三级光阑，前两级为圆光阑，第三级为矩形光阑，镜组采用凸透镜和整形透镜结合。激光器输出的光束经过前两级圆光阑后，可以滤除周围的杂散光，得到一个质量较高的圆光斑；然后经过凸透镜进行光源会聚，紧接着通过柱面透镜进行光斑整形，得到矩形光斑；最后经过第三级光阑，得到高质量的扁平矩形线光斑，如图 4(b)所示。原始光斑和处理后光斑的数据如表 1 所示。

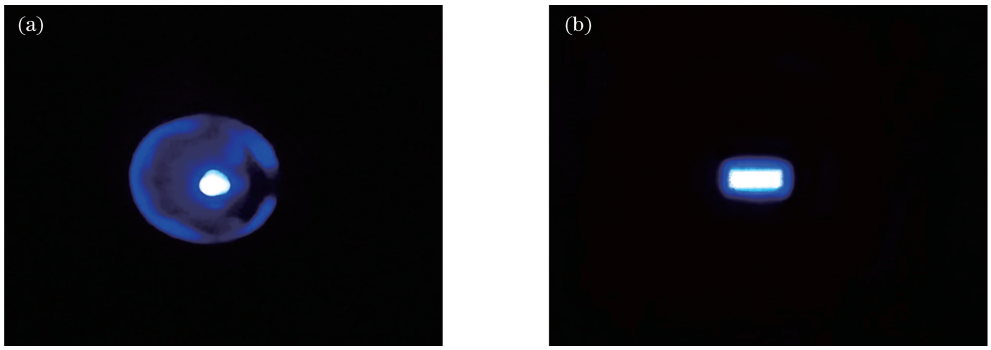

图 4　光斑形貌图。(a)激光器的原始输出光斑；(b)整形后的光斑

Fig. 4　Spot topography. (a) Original laser output spot; (b) shaping spot

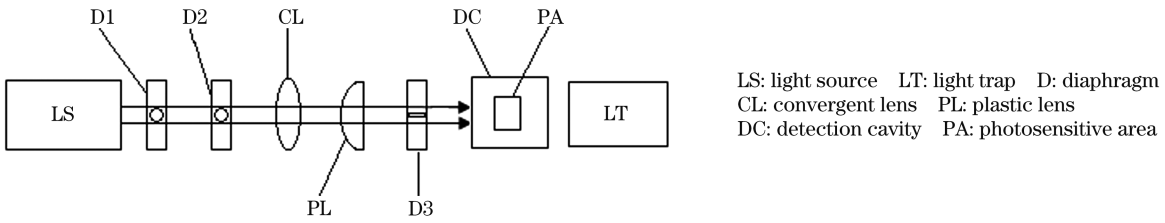

图 5　光学去噪光路

Fig. 5　Optical denoising light path

表 1　光斑数据

Table 1　Spot data

Name	Size of original spot /(mm×mm)	Size of processing spot /(mm×mm)
Center spot	2.5×3	1×3
Stray spot	12.5×15	1.5×3.5

4　结构设计

系统的光学检测腔体如图 6 所示，图 6(a)为检测腔结构的 3D 效果图，图 6(b)为检测腔结构的实物图。检测腔体材料为经氧化发黑处理的铝合金，其 6 个面分别连接光源、样本气体进气口、出气口、微生物粒子检测单元、凹面会聚镜以及光陷阱。

组装完成的检测装置如图 7 所示。

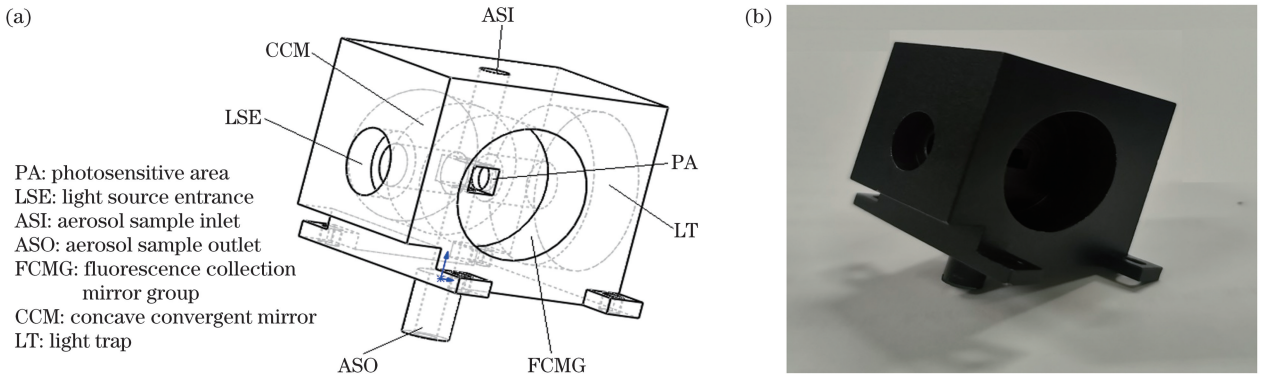

图 6　检测腔结构图。(a) 3D 效果图;(b)实物图

Fig. 6　Detecting cavity structure diagram. (a) 3D design sketch; (b) picture

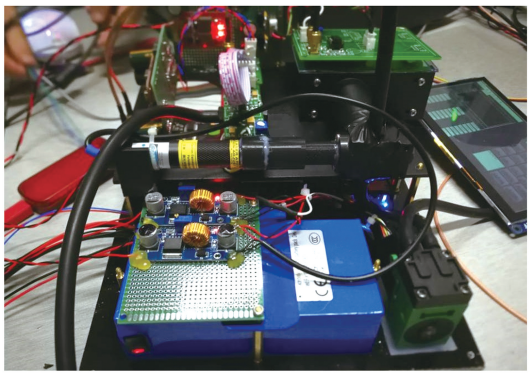

图 7　整体检测装置

Fig. 7　Overall detection device

5　性能测试与分析

实验中采用贝尔思 BSW-2A 超声雾化器将不同粒径的绿色荧光微球粒子的悬浮液进行雾化。经过滤膜过滤后,抽气泵将微球粒子送入光学检测区,采用示波器观察 PMT 的输出波形。

5.1　噪声分析

整个系统的噪声主要包含两部分,一是由杂散光引入的光学噪声,二是由电子元件和 PMT 引入的电学噪声。本文从光学和电学两方面对噪声进行抑制。图 8(a)是激光光源未进行整形直接照射到检测区后,PMT 输出的噪声信号,最大噪声超过了 120 mV。图 8(b)是通过前述设计的光路对激光输出光斑进行整形后,PMT 输出的噪声信号,最大噪声降至约 70 mV。由于噪声中的高频成分比较多,因此在 PMT 输出端增加了两级截止频率为 100 kHz 的 RC 滤波器,图 8(c)是测试结果,噪声降至约 20 mV。

可见,本文采用的两个方法可以有效抑制噪声,提高了信噪比。

5.2　检测性能测试

将粒径分别为10,5,2,1 μm的荧光微球(型号:

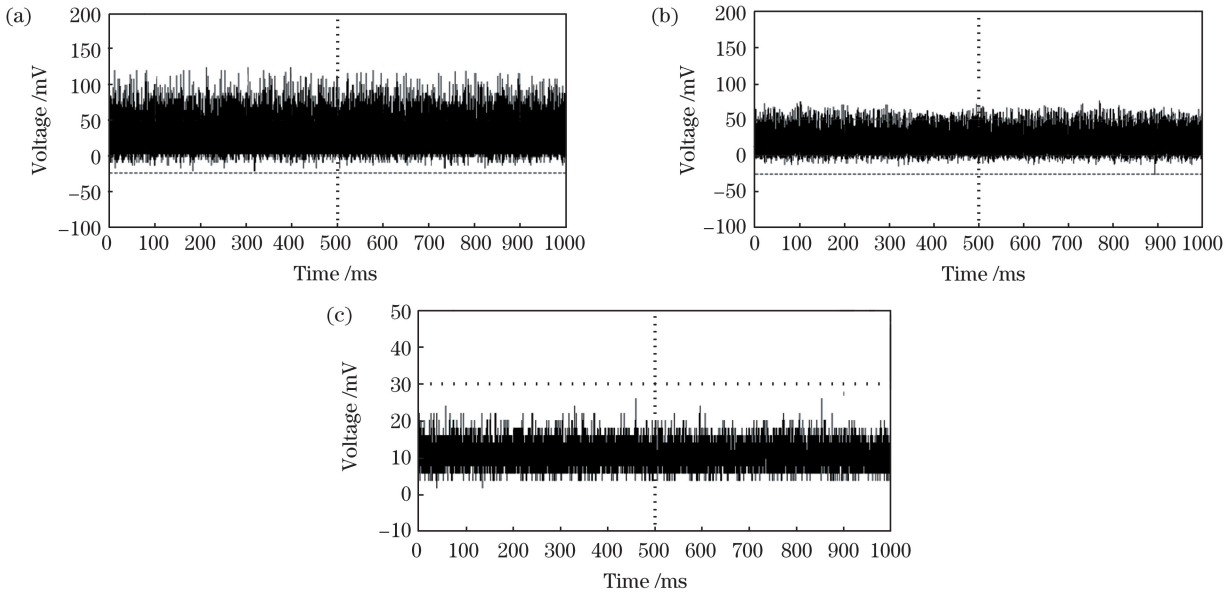

图 8　噪声信号。(a)未处理;(b)光学去噪处理后;(c)光学去噪和电学去噪处理后

Fig. 8　Noise signal. (a) Without treatment; (b) after optical denoising processing; (c) after optical denoising and electrical denoising processing

7-3-0100/0200/0500/1000)作为测试对象,该荧光微球购于天津倍思乐色谱技术开发中心,其在蓝光激发下发出绿色波段荧光。通过超声雾化器将荧光微球悬浮液雾化后进行检测,由于微球粒径不可能完全一致,所以对每个粒径均记录较大和较小的脉冲信号。

图 9 是 10 μm 荧光微球的测试电压信号,信号幅值为 350～380 mV。图 10 是 5 μm 荧光微球的测试电压信号,信号幅值为 250～290 mV。图 11 是 2 μm 荧光微球的测试电压信号,信号幅值为 130～140 mV。图 12 是 1 μm 荧光微球的测试电压信号,信号幅值为 78～90 mV。

测试结果表明,该光学系统可以有效检测到不同粒径荧光微球的信号,且信噪比较高,信号幅值与粒径的大小呈正相关。

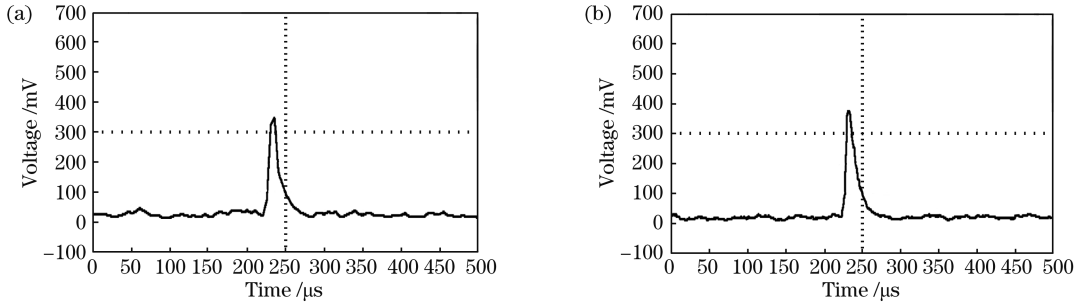

图 9 10 μm 荧光微球的荧光检测曲线。(a)峰值 350 mV ;(b)峰值 380 mV

Fig. 9 Fluorescence detection curve of 10 μm fluorescent microsphere. (a) Peak value of 350 mV; (b) peak value of 380 mV

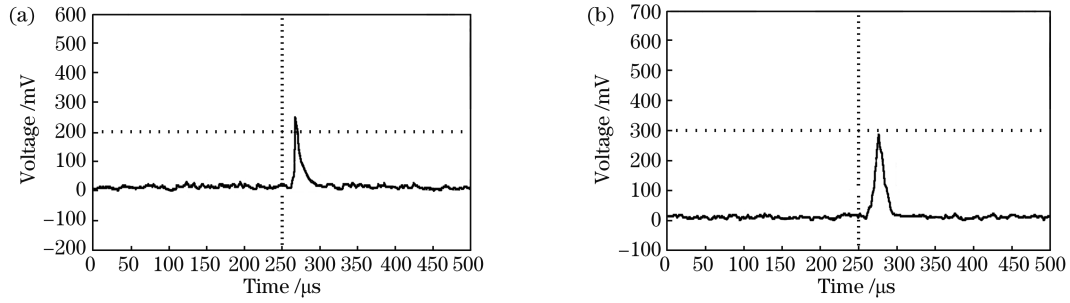

图 10 5 μm 荧光微球的荧光检测曲线。(a)峰值 250 mV;(b)峰值 290 mV

Fig. 10 Fluorescence detection curve of 5 μm fluorescent microsphere. (a) Peak value of 250 mV; (b) peak value of 290 mV

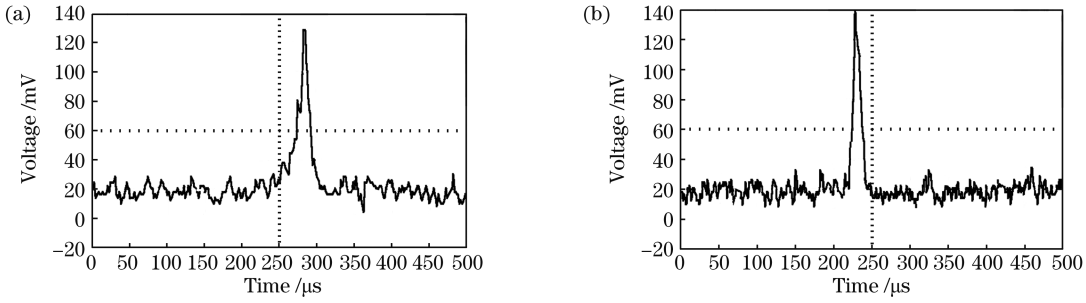

图 11 2 μm 荧光微球的荧光检测曲线。(a)峰值 130 mV;(b)峰值 140 mV

Fig. 11 Fluorescence detection curve of 2 μm fluorescent microsphere. (a) Peak value of 130 mV; (b) peak value of 140 mV

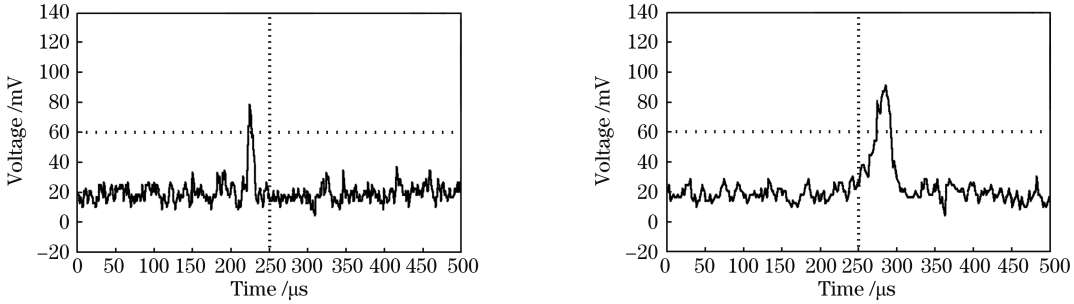

图 12 1 μm 荧光微球荧光检测曲线。(a)峰值 78 mV; (b)峰值 90 mV

Fig. 12 Fluorescence detection curve of 1 μm fluorescent microsphere. (a) Peak value of 78 mV; (b) peak value of 90 mV

6 结 论

本文设计了基于荧光检测技术的气溶胶微生物粒子计数仪的光学系统，并完成了该光学系统的设计和结构制造。

通过设计光学去噪光路，有效抑制了光学噪声，提高了系统的信噪比，系统的最终噪声仅约为 20 mV。

采用 10 μm 荧光微球、5 μm 荧光微球、2 μm 荧光微球和 1 μm 荧光微球对检测系统的性能进行了初步测试，测得的脉冲信号幅值分别为 350～380 mV、250～290 mV、130～140 mV 和 78～90 mV，说明系统的检测分辨力较好。

下一步拟对微生物样本，如金黄色葡萄菌、大肠杆菌等进行测试，并进一步优化系统结构，完成仪器的整体设计。

参 考 文 献

[1] Fleck R, Gill R L, Pettit T, et al. Characterisation of fungal and bacterial dynamics in an active green wall used for indoor air pollutant removal [J]. Building and Environment, 2020, 179: 106987.

[2] Harbizadeh A, Mirzaee S A, Khosravi A D, et al. Indoor and outdoor airborne bacterial air quality in day-care centers (DCCs) in greater Ahvaz, Iran[J]. Atmospheric Environment, 2019, 216: 116927.

[3] Liu H, Hu Z C, Zhou M, et al. Airborne microorganisms exacerbate the formation of atmospheric ammonium and sulfate [J]. Environmental Pollution, 2020, 263: 114293.

[4] Liu F W. Study of the laser induced fluorescence technology for detecting microorganisms [D]. Shanghai: Shanghai Institute of Technical Physics Chinese Academy of Sciences, 2014: 21-24.
刘方武. 激光诱导荧光微生物检测技术研究[D]. 上海: 上海技术物理研究所, 2014: 21-24.

[5] Zhu Q S, Hao S G, Luo N N, et al. Detection and quantification of vegetable oil adulteration based on laser-induced fluorescence spectroscopy[J]. Chinese Journal of Lasers, 2019, 46(12): 1211002.
朱泉水, 郝仕国, 罗宁宁, 等. 基于激光诱导荧光的植物油掺假检测与量化分析[J]. 中国激光, 2019, 46(12): 1211002.

[6] Xu X J, Wang X S, Li A Z, et al. Fast classification of tea varieties based on laser-induced breakdown spectroscopy[J]. Chinese Journal of Lasers, 2019, 46(3): 0311003.
徐向君, 王宪双, 李昂泽, 等. 基于激光诱导击穿光谱的茶叶品种快速分类[J]. 中国激光, 2019, 46(3): 0311003.

[7] Liang Z Y, Liu F. Research progress on real-time quantitative PCR technology and its application[J]. Modern Agricultural Science and Technology, 2020(6): 1-3,8.
梁子英, 刘芳. 实时荧光定量 PCR 技术及其应用研究进展[J]. 现代农业科技, 2020(6): 1-3,8.

[8] Liu T Z, Li X Q, Liu J J, et al. Detection of surface microbial count on elevator buttons of hospital using ATP bioluminescence method [J]. Journal of Integration Technology, 2015, 4(4): 82-86.
刘天钊, 李晓青, 刘俊江, 等. ATP 荧光检测法检测医院电梯按钮表面细菌总数[J]. 集成技术, 2015, 4(4): 82-86.

[9] Amodio E, Cannova L, Villafrate M R, et al. Analytical performance issues: comparison of ATP bioluminescence and aerobic bacterial count for evaluating surface cleanliness in an Italian hospital [J]. Journal of Occupational and Environmental Hygiene, 2014, 11(2): D23-D27.

[10] Ren L, Yang X X, Wei R L, et al. A novel fluorescence biosensor system for fluorescence detection of *E. coli*[J]. Journal of Anhui University (Natural Science Edition), 2019, 43(5): 97-102.
任乐, 杨席席, 韦瑞林, 等. 一种新颖的荧光生物传感系统对大肠杆菌的荧光检测[J]. 安徽大学学报(自然科学版), 2019, 43(5): 97-102.

[11] Zhang Y Y, Chen S T. Estimation of laser spot size in strong noise [J]. Science Technology and Engineering, 2012, 12(18): 4432-4434,4439.
张艳艳, 陈苏婷. 强噪声下激光光斑尺寸的估计[J]. 科学技术与工程, 2012,12(18): 4432-4434,4439.

[12] Mi Z, Cong C, Cheng Y, et al. Study on defects detection technique of precise optical element[C]// Proceedings of the Third International Conference on Energy and Environmental Research Progress (ICAEER 2018). [S. l.]: EDP Sciences, 2018: 01037.

[13] Yang Y R, Bu Y, Xu J H, et al. Measurement of surface defects of optical elements based on spectral estimation and multispectral technique[J]. Chinese Journal of Lasers, 2019, 46(9): 0904002.
杨言若, 步扬, 徐静浩, 等. 基于光谱估计与多光谱技术的光学元件表面疵病检测[J]. 中国激光, 2019, 46(9): 0904002.

[14] Li T R, Wang J F, Zhang X M, et al. Stray light analysis of the Xinglong 2.16-m telescope [J]. Research in Astronomy and Astrophysics, 2020, 20(3): 30.

[15] Chen L H, Yang G W, Liu Y X. Development of

semiconductor lasers[J]. Chinese Journal of Lasers, 2020, 47(5): 0500001.
陈良惠, 杨国文, 刘育衔. 半导体激光器研究进展[J]. 中国激光, 2020, 47(5): 0500001.

[16] Zhang L L, Chen Y, Wang C X, et al. Development and performance evaluation of portable 405 nm laser-induced fluorescence detector[J]. Applied Laser, 2019, 39(6): 1035-1040.
张玲玲, 陈媛, 王彩霞, 等. 便携式 405 nm 激光诱导荧光检测仪的研制和性能评估[J]. 应用激光, 2019, 39(6): 1035-1040.

[17] Cao Z, Long S, Lu F N, et al. Investigation of fluorescence spectrometry for determination of riboflavin in vitamin tablets[J]. Food & Machinery, 2009, 25(4): 95-99.
曹忠, 龙姝, 卢菲娜, 等. 荧光光谱分析法用于维生素药片中核黄素的检测[J]. 食品与机械, 2009, 25(4): 95-99.

[18] Bai T Z. The development of the laser induced fluorescence detection aerosol device and experiment results[D]. Hefei: University of Science and Technology of China, 2017: 1-4.
白同正. 激光诱导荧光探测气溶胶装置的研制及实验研究[D]. 合肥: 中国科学技术大学, 2017: 1-4.

[19] Fang Z Q, Chen G Q, Wu Y M. Study on the spectral properties of riboflavin in different polar solvents[J]. Spectroscopy and Spectral Analysis, 2020, 40(4): 1132-1136.
方梓秋, 陈国庆, 吴亚敏. 核黄素在不同极性溶剂中的光谱特性研究[J]. 光谱学与光谱分析, 2020, 40(4): 1132-1136.

[20] Xu A, Xiong C, Zhang P, et al. Research on dual-channel detection technology of bio-aerosols with intrinsic fluorescence measurement[J]. Acta Optica Sinica, 2013, 33(8): 0812005.
徐傲, 熊超, 张佩, 等. 基于本征荧光测量的双通道生物气溶胶检测技术研究[J]. 光学学报, 2013, 33(8): 0812005.

Design of Optical System of Aerosol Microbial Particle Counter

Zhang Zhiqiang[1,2], Song Fengmin[1], Zhang Qin[3,4], Dang Lei[3,4], Xu Yi[1], Li Shunbo[1**], Chen Li[1,2*]

[1] *Key Laboratory of Optoelectronic Technology & System (Chongqing University), Ministry of Education, Key Disciplines Laboratory of Novel Micro-Nano Devices and System Technology, College of Optoelectronic Engineering, Chongqing University, Chongqing* 400044, *China*;
[2] *State Key Laboratory of Transducer Technology, Chinese Academy of Sciences, Shanghai* 200050, *China*;
[3] *Aerospace Shenzhou Biotechnology Group Co., Ltd., Beijing* 100080, *China*;
[4] *Beijing Space Bioengineering Technology Research Center, Beijing* 100091, *China*

Abstract

Objective Recently, researchers increasingly focused on air quality. The air microorganisms cause severe harm to human health and severe effects on some industrial production. The latest national standard "Public Places Hygiene Indicators and Limits Requirements" stipulates the total number of air bacteria. Microbial detection based on fluorescence technology is widely used in medicine, pharmaceuticals, food, and environmental monitoring. The detection technologies include real-time fluorescent quantitative polymerase chain reaction (PCR), adenosine triphosphate (ATP) fluorescence detection, and microbial particle fluorescence-sensing system. The fluorescent microbial particle counter can directly count microbial particles, which has some advantages of good real-time performance, a high degree of automation, and simple operation. Besides, it is suitable for real-time online monitoring of the concentration of air microorganisms. This study designs a optical system based on the fluorescence detection principle in microbial particle counter to realize the online monitoring of microbial particles.

Methods The optical system is designed based on the fluorescence detection principle. In this study, the fluorescence characteristics of riboflavin, nicotinamide adenine dinucleotide, and other substances contained in microbial particles were tested and analyzed at first. Then, a 405 nm wavelength semiconductor laser was determined as the excitation light source. To reduce the output stray light of the laser, the light source shaping and fluorescence detection optical paths based on the combined diaphragm and lens were designed to obtain a high-quality flat rectangular line spot. Subsequently, consisting of oxidized and blackened aluminum alloy, the optical detection cavity structure were designed in the shape of hexahedron, and the production and assembly of the inspection

structure were completed. Finally, the performance of the optical detection system was tested and analyzed using fluorescent microspheres in different particle sizes.

Results and Discussions In this study, the fluorescence detection and analysis of two fluorescent substances, riboflavin and nicotinamide adenine dinucleotide, were first conducted. Under the excitation of blue light of the same wavelength, the fluorescence peak position of riboflavin is 541 nm [Fig. 1(a)]. The peak position of the fluorescence spectrum of adenine dinucleotide is 492 nm [Fig.1(b)]. Then, fluorescent microspheres were used to test the performance of the designed optical detection system. The results showed that the final output noise of the system was is about 20 mV [Fig. 8(c)], and it could achieve graded detection of 10, 5, 2, and 1 μm fluorescent microspheres. The test voltage signal of 10, 5, 2, and 1 μm fluorescent microspheres has a signal amplitude of 350–380 mV (Fig. 9), 250–290 mV (Fig. 10), 130–140 mV (Fig. 11), and 78–90 mV (Fig.12), respectively. The test results showed that the optical detection system can effectively detect the signals of fluorescent microspheres of different particle sizes and has the characteristics of high signal-to-noise ratio and high detection sensitivity, which is of great significance for the further development of aerosol microbial particle counting instruments.

Conclusions In this study, an aerosol microbial particle counting instrument optical system based on fluorescence detection technology was designed. The overall structure of the instrument optical system was proposed. Besides, the design and structure manufacturing of the optical system were completed. By designing optical denoising optical path, optical noise is effectively suppressed, and the system signal-to-noise ratio is improved. Combined with the second-order RC low-pass filter circuit, the final noise of the system is only about 20 mV. The performance of the detection system was preliminarily tested with 10, 5, 2, and 1 μm fluorescent microspheres. The measured pulse signal amplitudes were 350–380 mV, 250–290 mV, 130–140 mV and 78–90 mV; system detection resolution is better. Next, some microbial samples, such as *Staphylococcus aureus* and *Escherichia coil* will be tested, and further the structure will be optimized to complete the overall design of the instrument.

Key words Bio-optics; fluorescence; microbial particles; optical system; optical noise

OCIS codes 140.3460; 250.5230; 220.4830